



You have downloaded a document from  
**RE-BUŚ**  
repository of the University of Silesia in Katowice

**Title:** The influence of Nb atoms on the crystallization process of Fe-B-Nb amorphous alloys

**Author:** Rafał Babilas, Mariola Kądziołka-Gaweł

**Citation style:** Babilas Rafał, Kądziołka-Gaweł Mariola. (2011). The influence of Nb atoms on the crystallization process of Fe-B-Nb amorphous alloys. "Acta Physica Polonica A" Nr 2 (2015), s. 573-575.  
doi: 10.12693/APhysPolA.127.573



Uznanie autorstwa - Użycie niekomercyjne - Bez utworów zależnych Polska - Licencja ta zezwala na rozpowszechnianie, przedstawianie i wykonywanie utworu jedynie w celach niekomercyjnych oraz pod warunkiem zachowania go w oryginalnej postaci (nie tworzenia utworów zależnych).



UNIwersYTET ŚLĄSKI  
W KATOWICACH



Biblioteka  
Uniwersytetu Śląskiego



Ministerstwo Nauki  
i Szkolnictwa Wyższego

# The Influence of Nb Atoms on the Crystallization Process of Fe–B–Nb Amorphous Alloys

R. BABILAS<sup>a,\*</sup> AND M. KĄDZIOLKA-GAWEŁ

<sup>a</sup>Institute of Engineering Materials and Biomaterials, Silesian University of Technology,  
S. Konarskiego 18a, 44-100 Gliwice, Poland

<sup>b</sup>Institute of Physics, University of Silesia, Uniwersytecka 4, 40-007 Katowice, Poland

The ferromagnetic Fe-based amorphous alloys have been studied due to the attractive properties for soft magnetic applications. Depending on different Nb concentration, we studied the formation of crystalline phases in annealed samples of amorphous metallic alloys for  $\text{Fe}_{80-x}\text{B}_{20}\text{Nb}_x$  ( $x = 0, 4, 10$ ). The nature of the crystallization products as well as the phase structure were determined by using the Mössbauer spectrometry combined with X-ray diffraction and differential scanning calorimetry results. Substitution of Fe atoms by Nb lead to significant changes in hyperfine magnetic field ( $B_{\text{hf}}$ ) distributions in as-quenched amorphous alloys  $\text{Fe}_{80-x}\text{B}_{20}\text{Nb}_x$ , for  $x = 10$  the minimal value of  $B_{\text{hf}}$  is observed. Addition of this element causes shift of crystallization process towards higher temperatures and induces formation of phase complex including the  $\alpha$ -Fe,  $\text{Fe}_2\text{B}$  and  $\text{Fe}_3\text{B}$ . Combination of X-ray diffraction and Mössbauer spectroscopy is very useful method in studying the structural environment of Fe atoms on a nearest-neighbor length scale.

DOI: [10.12693/APhysPolA.127.573](https://doi.org/10.12693/APhysPolA.127.573)

PACS: 61.05.cp, 64.70.pe, 75.50.Bb, 75.50.Kj

## 1. Introduction

The Fe-B-Nb amorphous and nanocrystalline alloys have been widely examined during the last decade due to the attractive properties for soft magnetic applications. The required magnetic properties are usually large saturation magnetization, low coercive field, and high permeability [1].

Recently, alloys with different transition metals (Nb, Zr, Hf) have been studied with the aim to obtain better thermal stability and high glass-forming ability [2]. The previous studies in [3] show differences in the primary crystallization process leading to differences in the structure and formed phases. The formation of  $\alpha$ -Fe has been obtained to be responsible for better magnetic properties (higher magnetic permeability) rather than fully glassy alloys.

The aim of the paper is the structure analysis of  $\text{Fe}_{(80-x)}\text{B}_{20}\text{Nb}_x$  ( $x = 0, 4, 10$ ) metallic glasses in as-quenched state and after annealing using the X-ray diffraction (XRD), differential scanning calorimetry (DSC) and the Mössbauer spectroscopy methods. The Mössbauer spectroscopy is a very sensitive technique to detect the nearest neighbours of the resonant Fe atoms.

## 2. Experimental

The studies were performed on  $\text{Fe}_{80}\text{B}_{20}$ ,  $\text{Fe}_{76}\text{B}_{20}\text{Nb}_4$  and  $\text{Fe}_{70}\text{B}_{20}\text{Nb}_{10}$  metallic glasses in the form of ribbons with the thickness of 0.03 mm and the width of 5 mm. The ingots of studied alloys were prepared by induction

melting of the mixtures of all pure elements together: Fe (99.98%), B (99.9%), Nb (99.95%) in nominal compositions. The amorphous ribbons were prepared by the “chill-block melt spinning” (CBMS) technique, which is a method of continuous casting of the liquid alloy on the surface of a turning copper based wheel [4, 5]. The casting conditions include linear speed of copper wheel of 20 m/s and ejection over-pressure of molten alloy under Ar of 0.04 MPa.

The structure of the samples in “as-quenched” states and after crystallization was examined by XRD in reflection mode using the Seifert-FPM XRD 7 diffractometer with  $\text{Co } K_{\alpha}$  radiation. The diffraction patterns were collected by “step-scanning” method in the  $2\theta$  range from  $30^{\circ}$  to  $90^{\circ}$ . The crystallization analysis associated with the onset ( $T_x$ ) and the peak crystallization ( $T_p$ ) of studied samples were determined by the DSC method using the DuPont 910 device in the temperature range from 600 to 950 K and a constant heating rate of 20 K/min under the argon atmosphere.

The  $^{57}\text{Fe}$  Mössbauer spectra were recorded at room temperature using a constant acceleration spectrometer with triangular velocity shape, a multichannel analyzer with 1024 channels, and linear arrangement of the  $^{57}\text{Co}(\text{Cr})$  source ( $\approx 15$  mCi), absorber and detector. The spectrometer velocity was calibrated with a high purity  $\alpha$ -Fe foil. All spectra were fitted by means of a hyperfine field distribution using the Hesse-Rübartsch procedure with linear correlation between isomer shift and hyperfine magnetic field.

## 3. Results and discussion

The amorphous structure of studied Fe-based alloys in as-quenched state was firstly examined by XRD method. The diffraction patterns of studied samples show the

\*corresponding author; e-mail: [rafal.babilas@polsl.pl](mailto:rafal.babilas@polsl.pl)

broad diffraction halo, which is characteristic for the amorphous materials with disordered atomic structure (Fig. 1).

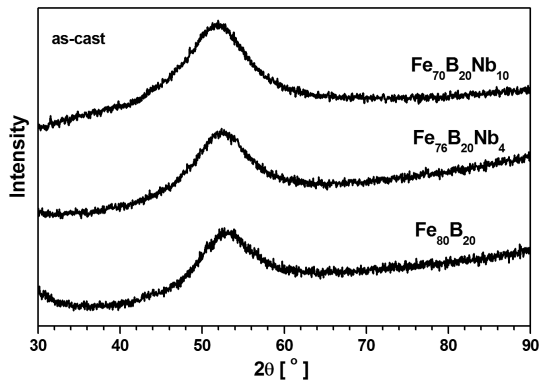


Fig. 1. X-ray diffraction patterns of studied  $\text{Fe}_{80}\text{B}_{20}$ ,  $\text{Fe}_{76}\text{B}_{20}\text{Nb}_4$  and  $\text{Fe}_{70}\text{B}_{20}\text{Nb}_{10}$  samples in as-quenched state.

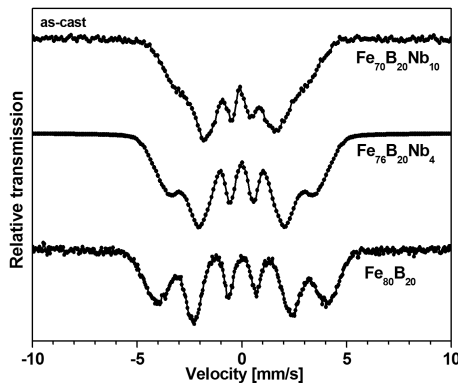


Fig. 2. Mössbauer spectra of studied metallic glasses.

Figure 2 shows room temperature Mössbauer spectra obtained for alloys in as-quenched state. The spectra show broadened sextet patterns typical for the structural disorder of amorphous ferromagnetic materials. The values of the average hyperfine magnetic field ( $B_{\text{hf}}$ ) as well as the isomer shift ( $IS$ ) parameters were obtained for the best fitting (Table I). Substitution of Fe atoms by Nb leads to significant changes in hyperfine magnetic field ( $B_{\text{hf}}$ ) distributions, for  $\text{Fe}_{70}\text{B}_{20}\text{Nb}_{10}$  the minimal value of  $B_{\text{hf}}$  is observed. The  $IS$  parameter is also changed after Nb addition.

TABLE I

Average values of isomer shift ( $IS$ ) and hyperfine magnetic field ( $B_{\text{hf}}$ ) of  $\text{Fe}_{(80-x)}\text{B}_{20}\text{Nb}_x$  metallic glasses in as-quenched state.

Glassy alloy	$IS$ [mm/s]	$B_{\text{hf}}$ [T]
$\text{Fe}_{80}\text{B}_{20}$	0.071	24.6
$\text{Fe}_{76}\text{B}_{20}\text{Nb}_4$	0.092	18.6
$\text{Fe}_{70}\text{B}_{20}\text{Nb}_{10}$	0.039	15.2

DSC curves of studied glassy alloys prepared by melt spinning are presented in Fig. 3. The exothermic peaks describing a single stage of crystallization are observed

for all samples. It is seen that  $T_x = 682$  K and  $T_p = 706$  K achieved the lowest value for basic  $\text{Fe}_{80}\text{B}_{20}$  alloy. The addition of 4 at.% Nb to binary alloy caused the increase of  $T_x$  to 817 K and  $T_p$  to 819 K. Moreover, the increase of Nb content up to 10 at.% caused the increase of  $T_x$  and  $T_p$  which reached 832 K and 845 K, adequately.

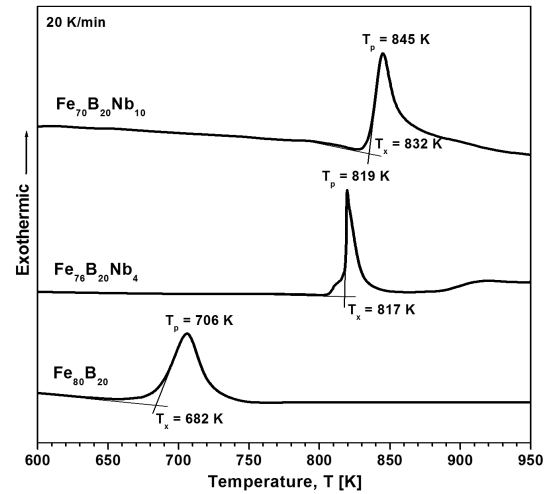


Fig. 3. DSC curves of examined amorphous ribbons.

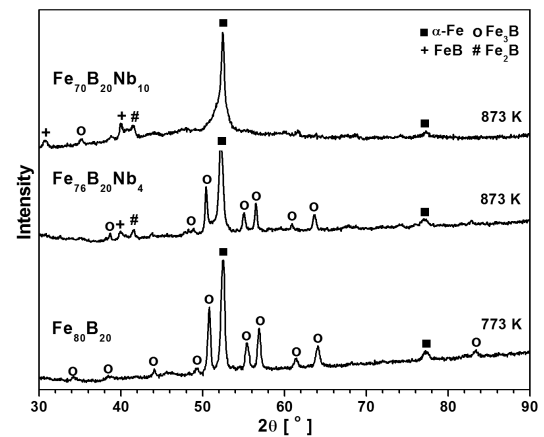


Fig. 4. X-ray diffraction patterns of studied  $\text{Fe}_{80}\text{B}_{20}$ ,  $\text{Fe}_{76}\text{B}_{20}\text{Nb}_4$  and  $\text{Fe}_{70}\text{B}_{20}\text{Nb}_{10}$  alloys after annealing at 773 and 873 K/1 h.

Figure 4 shows XRD patterns obtained for studied alloys after annealing for 1 h at 773 K for Fe–B and 873 K for Fe–B–Nb alloys. The temperature of annealing for each alloy is higher than  $T_p$  obtained by DSC method. Qualitative phase analysis from X-ray data enables the identification of  $\alpha$ -Fe phase and iron borides —  $\text{Fe}_3\text{B}$  for samples of  $\text{Fe}_{80}\text{B}_{20}$  alloy. The annealing at temperature of 873 K obviously caused a formation of crystalline  $\alpha$ -Fe and iron borides —  $\text{FeB}$ ,  $\text{Fe}_2\text{B}$  and  $\text{Fe}_3\text{B}$ .

The Mössbauer spectra obtained for annealed samples indicate the presence of  $\text{Fe}_3\text{B}$  with  $\alpha$ -Fe in all alloys (Figs. 5–7). The experimental spectrum of crystalline  $\text{Fe}_{80}\text{B}_{20}$  alloy was fitted with four sextets, three corresponding to  $\text{Fe}_3\text{B}$  and one to  $\alpha$ -Fe. However, the spectrum obtained for  $\text{Fe}_{70}\text{B}_{20}\text{Nb}_{10}$  was fitted with eight

sxtets which include a singlet for the Fe–B and Fe–Nb paramagnetic phase, two sextets for Fe<sub>2</sub>B, three for Fe<sub>3</sub>B and one for  $\alpha$ -Fe. The values of the hyperfine field as well as the isomer shift and area from the spectra can be seen in Table II.

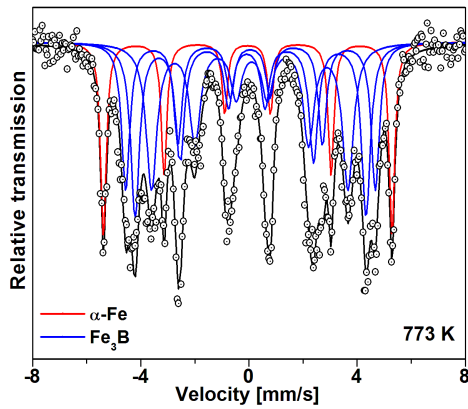


Fig. 5. Transmission Mössbauer spectrum and fittings of Fe<sub>80</sub>B<sub>20</sub> metallic glass after annealing at 773 K/1 h.

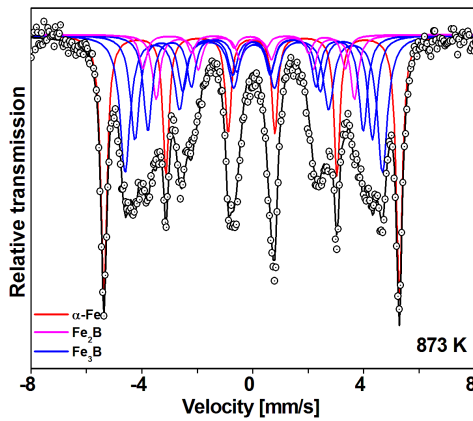


Fig. 6. Transmission Mössbauer spectrum and fittings of Fe<sub>76</sub>B<sub>20</sub>Nb<sub>4</sub> metallic glass after annealing at 873 K/1 h.

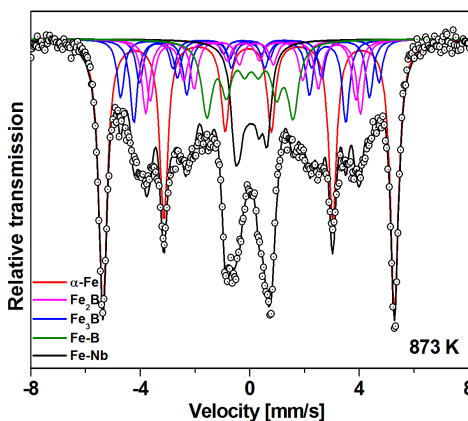


Fig. 7. Transmission Mössbauer spectrum and fittings of Fe<sub>70</sub>B<sub>20</sub>Nb<sub>10</sub> metallic glass after annealing at 873 K/1 h.

The alloy containing 10 at.% Nb shows better performance against crystallization than material without Nb addition and with 4 at.% of niobium.

TABLE II

Hyperfine parameters of Fe<sub>(80-x)</sub>B<sub>20</sub>Nb<sub>x</sub> alloys annealed at 773 and 873 K/1 h (*IS* — isomer shift, *B<sub>hf</sub>* — hyperfine magnetic field, *A* — relative area from the spectra).

Glassy alloy	<i>IS</i> [mm/s]	<i>B<sub>hf</sub></i> [T]	<i>A</i> [%]	Phase
Fe <sub>80</sub> B <sub>20</sub> 773 K	0.098 ± 0.005	28.7 ± 0.05	80	Fe <sub>3</sub> B
	0.037 ± 0.004	26.7 ± 0.05		
	0.114 ± 0.005	22.6 ± 0.04	20	$\alpha$ -Fe
Fe <sub>76</sub> B <sub>20</sub> Nb <sub>4</sub> 873 K	-0.155 ± 0.017	22.7 ± 0.11	19	Fe <sub>2</sub> B
	0.114 ± 0.006	24.2 ± 0.06		
	0.146 ± 0.010	22.3 ± 0.08	52	Fe <sub>3</sub> B
0.042 ± 0.006	26.7 ± 0.06			
Fe <sub>70</sub> B <sub>20</sub> Nb <sub>10</sub> 873 K	0.089 ± 0.004	28.9 ± 0.05	29	$\alpha$ -Fe
	0.002 ± 0.001	33.2 ± 0.01		
	0.068 ± 0.006	3.7 ± 0.04	11	Fe–Nb
Fe <sub>70</sub> B <sub>20</sub> Nb <sub>10</sub> 873 K	0.083 ± 0.008	9.8 ± 0.10	13	Fe–B
	-0.008 ± 0.007	23.4 ± 0.12		
	0.227 ± 0.006	24.4 ± 0.09	18	Fe <sub>2</sub> B
	-0.162 ± 0.005	24.1 ± 0.11		
	0.089 ± 0.009	27.2 ± 0.06	22	Fe <sub>3</sub> B
	-0.041 ± 0.006	28.3 ± 0.05		
-0.001 ± 0.001	33.1 ± 0.10	36	$\alpha$ -Fe	

#### 4. Conclusions

The Mössbauer spectra of studied metallic glasses are typical for amorphous ferromagnetic materials, but showed remarkable changes with niobium addition. The increase of Nb concentration leads to decrease of average hyperfine magnetic field and isomer shift. The addition of Nb to Fe–B alloys causes shift of crystallization process towards higher temperatures and induces formation of phase complex including the  $\alpha$ -Fe, Fe<sub>3</sub>B and Fe<sub>2</sub>B in addition.

#### Acknowledgments

The work was supported by National Science Centre under research project no.: 2011/03/D/ST8/04138.

#### References

- [1] M.E. McHenry, M.A. Willard, D.E. Laughlin, *Prog. Mater. Sci.* **44**, 291 (1999).
- [2] S.N. Kane, A. Gupta, Zs. GerCSI, F. Mazaleyrat, L.K. Varga, *J. Magn. Magn. Mater.* **292**, 447 (2005).
- [3] J. Torrens-Serra, J. Rodriguez-Viejo, M.T. Clavaguera-Mora, *J. Non-Cryst. Solids* **353**, 842 (2007).
- [4] R. Nowosielski, R. Babilas, G. Dercz, L. Pająk, *Diffus. Def. Data B* **163**, 165 (2010).
- [5] R. Babilas, R. Nowosielski, W. Pilarczyk, G. Dercz, *Diffus. Def. Data B* **203-204**, 288 (2013).